Efficient Text Color Modulation for Printed Side Communications and Data Hiding

Paulo Vinicius Koerich Borges, Ebroul Izquierdo
Queen Mary, University of London
Multimedia and Vision Research Group
London, UK
vini@ieee.org, ebroul.izquierdo@elec.qmul.ac.uk

Joceli Mayer
Federal University of Santa Catarina
Digital Signal Processing Research Lab
Florianopolis, SC, Brazil
mayer@eel.ufsc.br

Abstract

This paper improves the use of text color modulation (TCM) as a reliable text document data hiding method. Using TCM, the characters in a document have their color components modified (possibly unperceptually) according to a side message to be embedded. This work presents a detection metric and an analysis determining the detection error rate in TCM, considering an assumed print and scan (PS) channel model. In addition, a perceptual impact model is employed to evaluate the perceptual difference between a modified and a non-modified character. Combining this perceptual model and the results from the detection error analysis it is possible to determine the optimum color modulation values. The proposed detection metric also exploits the orientation characteristics of color halftoning to reduce the error rate. In particular, because color halftoning algorithms use different screen orientation angles for each color channel, this is used as an effective feature to detect the embedded message. Experiments illustrate the validity of the analysis and the applicability of the method.

1. Introduction

Video, telephone, and Internet based communications have increased remarkably in the last few years. However, communication over paper still remains an essential mean of conveying information. Very often, important paper copies of documents are exchanged between companies and people. As a consequence, several methods have been proposed aiming at reliably authenticating hardcopy documents.

This paper investigates the use of TCM [8] as an efficient document authentication method. Using TCM, each individual character has its color modulated from the standard black to a different color. This modulation is performed, possibly unperceptually to the human eye, according to a side message to be embedded in the document. This is illustrated in Fig. 1, where c is the original image and s is image watermarked according to bit string $\mathbf{b}$. Detection is performed with the use of a scanner. Notice that it is not the goal of this paper to discuss the usefulness of TCM and related methods such as text luminance modulation (TLM), in which only the luminance of the characters are modified. This issue and practical implementation aspects have already been discussed in the literature [8, 13, 5].

In contrast, based on the TCM approach, this work provides the following contributions:

Figure 1. Example of text watermarking through TCM.

(i) Considering a PS channel model, a detection metric for TCM is proposed, which combines information of different color channels. For this metric, an analysis to estimate the theoretical error rate is presented. The Bhattacharyya bound [9] is used to determine the error probability when the information from the blue and red channels are combined.

(ii) The use of the CIE L*a*b* perceptual color space [1] is proposed, in order to determine the perceptual impact of the modulation in each color channel.

(iii) Using the error analysis and the perceptual impact results, an optimum modulation level is achieved, considering a tradeoff between error rate and perceptual impact.

(iv) In color printing, each color channel is printed in a given orientation angle to minimize the interference between color channels [2]. This is exploited in this paper, as the detection of the dominant angle in each character is also used to help identifying the type of color modulation employed, reducing the error rate.

This paper is organized as follows. Section 2 describes a PS channel, which is used in the error rate analysis. Section 3 proposes the detection metric to extract the embedded symbol from the character, providing an analysis to determine the error rate for the metric. Section 4 discusses the perceptual impact caused by TCM. Section 5 determines the optima modulation levels for a given detection error probability. Section 6 presents a metric to determine the dominant halftone orientation angle. Section 7 presents several experiments, validating the analysis and illustrating the applicability of the method. The paper closes with relevant conclusions in Section 8.

2. The Color Print and Scan Channel

Under a communications perspective, the PS process can be viewed as a noisy communication channel. In this work the PS channel model described in [5] is used, extended to the color case. For a given color channel C, $C \in \{R, G, B\}$ (where R, G and B stand for red, green and blue channels, respectively) the digital scanned image y_C is represented by

$$y_C(m,n) = g_{s_C}\Big\{\big\{g_{pr_C}[b_C(m,n)] + \eta_{1_C}(m,n)\big\}* \\ * h_{ps}(m,n)\Big\} + \eta_{3_C}(m,n), \tag{1}$$

where b_C is the halftoned image (corresponding to color channel C) generated from the original image s and η_{1_C} represents printing noise due to microscopic ink and paper imperfections. The noise η_{3_C} combines illumination and CCD electronic noise [7], as well as the quantization noise due to A/D. The operator * represents the convolution operation and h_{ps} represents a low-pass filter combining the point-spread functions of the printer and of the scanner. In the printing process, blurring occurs due to toner or ink spread. In the scanning process, the low-pass effect is due to the optics and the motion blur caused by the interactions between adjacent CCD arrays elements [7].

The terms $g_{pr_C}(\cdot)$ and $g_{s_C}(\cdot)$ in (1) represent gains in the printing and scanning processes, respectively. A detailed description of the other effect in this PS channel can be found in [5].

3. The Detection Process

In this section a detection metric is proposed and an analysis for the error rate is provided. Statistical and distortion assumptions for the analyses are discussed in Section 3.1. For simplicity, the (m, n) coordinate system is mapped to a one dimensional notation, and the index i is dropped from c_i and its derivations.

3.1. Statistical and Distortion Assumptions

In the model in (1), it is possible to decompose b_C into a constant term $\bar{b_C}$ plus a noise term η_{2_C}, such that $b_C(n) = \bar{b_C} + \eta_{2_C}(n)$, where $\eta_{2_C}(n)$ is the quantization noise. The variance of the quantization noise depends on the average level $\bar{b_C}$. It is given by

$$\sigma^2_{\eta_{2_C}} = \bar{b_C} - (\bar{b_C})^2. \tag{2}$$

A proof of this equality and a complete characterization of the noise η_{2_C} is given in [5].

Considering a low perceptual impact requirement in the modulation process, the detector operates in a small range of the luminance range $[0, 1]$ of each color channel. For this reason, g_{s_C} in (1) can be approximated to a linear model [7] and g_{s_C} is approximated to 1 for simplicity. Assuming that b_C is generated from a constant color region, that is, $b_C(n) = b_{0_C} = \bar{b_C}$, where b_{0_C} is the average color of the modulated character prior to printing, (1) can be written as (using an one-dimension notation)

$$y_C(n) = \big\{\alpha_C[b_{0_C} + \eta_{2_C}(n)] + \eta_{1_C}(n)\big\} * h_{ps}(n) + \eta_{3_C}(n), \tag{3}$$

The term α_C represents a gain (see g_{pr_C} in (1)) that varies slightly throughout a full page due to non-uniform printer toner distribution. Due to its slow rate of change, α_C is modeled as constant in n but it varies with each realization i satisfying $\alpha_C \sim \mathcal{N}(\mu_{\alpha_C}, \sigma^2_{\alpha_C})$, where i represents the $i-$th character in TCM watermarking.

Due to the nature of the noise (discussed in Section 2) and based on experimental observations, η_{1_C} and η_{3_C} can be generally modeled as zero-mean mutually independent Gaussian noise [7, 12].

3.2. Detection Metric

Human vision experiments illustrate that variations in the green channel are more easily perceived than variations in the red and blue channels [11, 10]. This is supported by experiments performed in this paper. For this reason, a modulation scheme which modifies only the blue and red channels is used in this work. The green channel is used as a reference. This increases the robustness of the method, as

illumination variations and scanner and printing gains affect all the channels. Based on the characteristics of the observed printed and scanned characters, the proposed detection metric is given by

$$\mathbf{d} = [d_b \quad d_r]^\top \tag{4}$$

where $\top$ represents the transpose operation and

$$d_b = d_B - d_G \tag{5}$$

where

$$\begin{aligned} d_B = \frac{1}{N}\sum_{n=1}^{N} y_B(n) = \frac{1}{N}\sum_{n=1}^{N}\big\{\alpha_B[w_B + \eta_{2B}(n)] \\ + \eta_{1B}(n)\big\} * h_{ps}(n) + \eta_{3B}(n), \end{aligned} \tag{6}$$

represents the average value in the blue channel after printing and w_B represents the modulation level in the blue channel prior to printing, such that $b_B = w_B$. Similarly, d_G represents the average value in the green channel. α represents and offset gain that varies from character to character [5]. A statistical analysis shows that the expected value μ_{d_b} and the variance $\sigma^2_{d_b}$ of d_b are given by

$$\mu_{d_b} = E\{d_b\} = E\{d_B - d_G\} = \mu_{\alpha_B} w_B - \mu_{\alpha_G} w_G \tag{7}$$

and

$$\begin{aligned} \sigma^2_{d_b} = \frac{(\sigma^2_{\alpha_B} + \mu^2_{\alpha_B})\sigma^2_{\eta_{2B}} + \sigma^2_{\eta_{1B}} + \sigma^2_{\eta_{3B}}}{N} \\ + \frac{(\sigma^2_{\alpha_G} + \mu^2_{\alpha_G})\sigma^2_{\eta_{2G}} + \sigma^2_{\eta_{1G}} + \sigma^2_{\eta_{3G}}}{N} \\ + w_B^2\sigma^2_{\alpha_B} + w_G^2\sigma^2_{\alpha_G}, \end{aligned} \tag{8}$$

where $\sigma^2_{\eta_{2B}} = (w_B - w_B^2)$.

First, assume that the detection is performed using only the blue channel, for example. Considering the $S = 2$ (or 1 bit) case, for example, the conditional error probability p_{01} of receiving a bit 0 given that bit 1 was transmitted is described by $p_{01} = \Pr(d_b > \lambda_B | \text{bit} = 1)$, where λ_b is a decision threshold. Defining the complementary error function $\text{erfc}(x) = \frac{2}{\sqrt{\pi}}\int_x^\infty e^{-t^2}dt$, $p_{01} = \frac{1}{2}\text{erfc}\left(\frac{\lambda_b - \mu_{d_b/1}}{\sqrt{2\sigma^2_{d_b/1}}}\right)$, where $\mu_{d_b/1}$ and $\sigma^2_{d_b/1}$ are respectively the mean and the variance of d_b for bit 1. Equivalently, if bit 0 is transmitted, the conditional error probability is given by $p_{10} = \frac{1}{2}\text{erfc}\left(\frac{\mu_{d_b/0} - \lambda_b}{\sqrt{2\sigma^2_{d_b/0}}}\right)$, where $\mu_{d_b/0}$ and $\sigma^2_{d_b/0}$ are respectively the mean and the variance of d_b for bit 0. Finally, the average error probability is expressed by

$$P_{e_{d_b}} = P_0 p_{10} + P_1 p_{01} \tag{9}$$

where P_0 and P_1 are the probabilities of occurrence of bits 0 and 1, respectively. A similar approach is valid for the red channel.

3.3. Bhattacharyya Bound on the Error Rate

To reduce the error rate, the metric d_b and d_r of the blue and red channels described in (4) are combined into a single metric. For this task, the Bayes decision rule is employed in this work. Because the metrics are assumed normally distributed, the Bayes decision rule guarantees the lowest average error rate [9].

An upper bound on the error rate is given by the Bhattacharyya bound for Gaussian variables [9]. Therefore, the classification error probability is:

$$P_{e_{\mathbf{d}}} = \sqrt{P_0 P_1}\, e^{-k} \tag{10}$$

where k is given by

$$\begin{aligned} k = \frac{1}{8}(\mu_{\mathbf{d}/1} - \mu_{\mathbf{d}/0})^T \left(\frac{\boldsymbol{\Sigma}_{/0} + \boldsymbol{\Sigma}_{/1}}{2}\right)^{-1} (\mu_{\mathbf{d}/1} - \mu_{\mathbf{d}/0}) \\ + \frac{1}{2}\ln\frac{\left|\frac{\boldsymbol{\Sigma}_{/0} + \boldsymbol{\Sigma}_{/1}}{2}\right|}{\sqrt{|\boldsymbol{\Sigma}_{/0}||\boldsymbol{\Sigma}_{/1}|}} \end{aligned} \tag{11}$$

where $\boldsymbol{\Sigma}_{/0}$ and $\boldsymbol{\Sigma}_{/1}$ represent the covariance matrices corresponding to bit 0 and bit 1, respectively.

Notice that k depends on the results from (7) and (8). Applying (11) to (10), the plot presented in Fig. 2 is generated. This figure illustrates the upper bound on the error rate given in (10) as a function of the modulation level in the red and blue channels, given by w_R and w_B, respectively. The noise parameters for generating this plot are given in the experiments section.

Notice that modulating both color channels yields a lower error rate than modulating only one color channel, at the expense of increased perceptual impact. The perceptual impact caused by the color modulation is discussed in the next section.

4. Perceptual Evaluation of Color Modulation

Using the CIELAB color difference metric discussed in [14], it is possible to estimate the perceptual impact of the modulation level, as the original image color is black (black characters). The perceptual distortion metric D is given by:

$$D = \sqrt{(L_0 - L)^2 + (a_0 - a)^2 + (b_0 - b)^2} \tag{12}$$

where L_0, a_0 and b_0 represent the parameters of the original color in the $L^*a^*b^*$ color space.

The graph in Fig. 3 shows the perceptual difference D between black and a color generated by the modulation of the blue and red channels. In this figure, the green channel is not modulated.

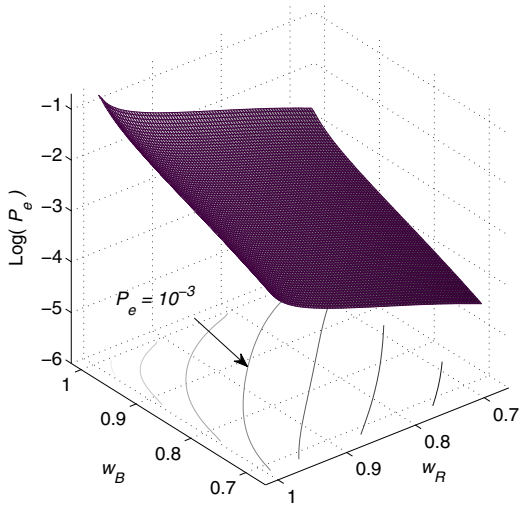

Figure 2. Bhattacharyya upper bound on the error probability using the Bayes classifier, as a function of the modulation in the red and blue channels.

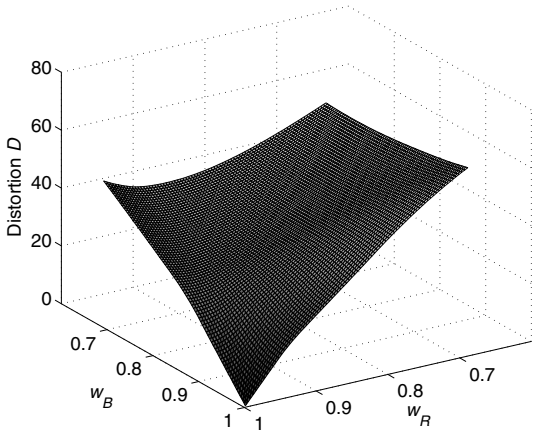

Figure 3. Perceptual impact based on the CIELAB color space caused by the character color modulation, as a function of the modulation in the red and blue channels.

5. Optimum Modulation Level Considering Error Probability and Perceptual Impact

Considering the least perceptual modulation (from Section 4) for a given error rate (from Section 3.3), the following optimization is performed

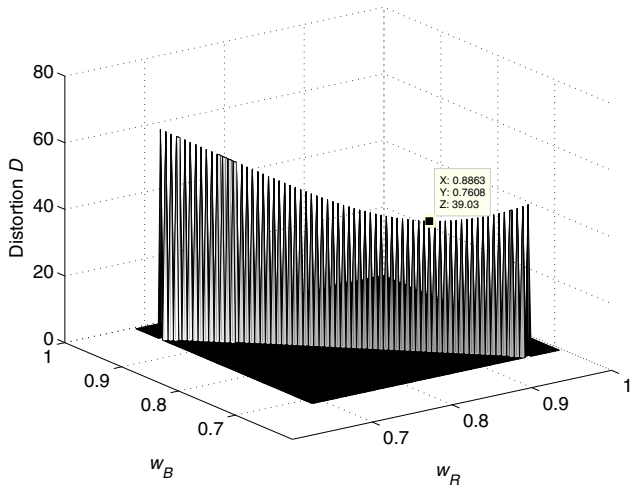

Figure 4. Illustration of the distortion as a function of w_B and w_R, considering an error probability $P_e = 0.0001$.

$$\underset{w_B, w_R \in [0,1] | P_{e_\mathbf{d}} = P'}{\operatorname{argmin}} D(w_B, w_R) \tag{13}$$

which returns the values w_B and w_R for which the distortion D is minimum, constrained to an error probability equal to $P_{e_\mathbf{d}} = P'$. This optimization process cannot be performed analytically. Instead, the modulation values which correspond to P' are tested regarding the distortion given in (12), where the minimum value is chosen as optimum.

Fig. 4 illustrates the distortion curve as a function of the modulation w_B and w_R, for an error probability upper bound equal to $P_{e_\mathbf{d}} = 0.0001$, based on the plot given in Fig. 2. Notice that when the distortion parameters of PS channel used are obtained, the error rates are obtained via (11) and the modulation levels that cause the least distortion (according to (12)) can be employed.

6. Auxiliary Metric to Improve Detection

In color printing, the dithering matrices for each channel are rotated to be as far apart in angle as possible. This rotation is usually set to $0°$ for the Y screen, $15°$ for the M screen, $45°$ for the K screen, and $75°$ for the C screen. This is illustrated in Fig. 5, which shows a halftone test target, extracted from 'The Londoner' newspaper. Therefore, when a character suffers color modulation, an "orientation modulation" also occurs as a consequence. This section proposes

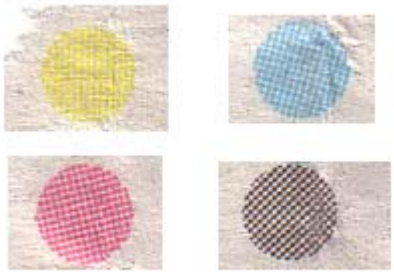

Figure 5. Example of color halftoning test targets, illustrating the C, M, Y and K colorants.

to use this characteristic as an auxiliary metric to help improving the detection in TCM.

Because the expected screen angle is known, the use of a directional edge detection filter "matched in angle" is a simple and efficient solution. The average energy of the filtered version of the character is an efficient discrimination metric to determine the predominant screen angle, therefore determining whether or not the character is color modulated. The maximum energy is attained when the filtering angle is set to 90° to the predominant screen angle of the modulated character, as the filtered patterns energies vary depending on the color used. The experiments illustrate the applicability of this type of detection.

7. Experiments

This section presents Monte Carlo simulations to illustrate the applicability of TCM and the reduced error rate when using the Bayes classifier to combine the color channels. It also presents experiments to validate the error rate analyses derived in Section 3, in addition to comparative results between TLM and TCM.

As expected, it was noticed that the distortion parameters and the noise in the PS channel vary according to the color channel and the printing and scanning devices used. The printing and scanning resolutions were set to 600 and 300 dots/inch and pixels/inch, respectively. The experiments were conducted with printers HP IJ-855C and Ricoh aficio 2238c, HP SJ-5P and Canon CanoScan LiDE 20. Typical values for the parameters in (1) are $\sigma_{\eta_{1R}} = 0.015$, $\sigma_{\eta_{3R}} = 0.012$, $\mu_{\alpha_R} = 0.83$, $\sigma_{\alpha_R} = 0.04$, for the red channel, $\sigma_{\eta_{1G}} = 0.02$, $\sigma_{\eta_{3G}} = 0.01$, $\mu_{\alpha_G} = 0.85$, $\sigma_{\alpha_G} = 0.03$, for the green channel, and $\sigma_{\eta_{1B}} = 0.015$, $\sigma_{\eta_{3B}} = 0.01$, $\mu_{\alpha_B} = 0.82$, $\sigma_{\alpha_B} = 0.03$, for the blue channel.

The remaining noise terms $\sigma^2_{\eta_{2R}}$ and $\sigma^2_{\eta_{2B}}$ are level dependent and are given by $\sigma^2_{\eta_{2B}} = w_B - w_B^2$ and $\sigma^2_{\eta_{2R}} = w_R - w_R^2$, as presented in (2), in Section 3.1.

These values were estimated using test targets of different colors, analyzing only the corresponding color channel. If different PS devices are used, a new parameter estimation is necessary if the user wishes to determine the theoretical error rate using (9).

To model the low-pass effect of the PS channel represented by h_{ps} in (1), the filter described in [3] is used in this paper, which is a Butterworth filter of order 1 and cutoff frequency equal to 0.17. Using the noise, gain and blurring filter parameters described above, a character distorted with the proposed PS model is perceptually similar to an actual printed and scanned character.

7.1. Experiment 1: Blue Channel Modulation

Consider the 1 bit/element case ($S = 2$). A large sequence of $K = 30360$ characters (as in 'abcdef...') is printed, with font type 'Arial', size 12 points. In the experiments small text elements such as commas and dots are not watermarked. Due to the small number of pixels in these elements, they are more susceptible to segmentation and detection errors.

Prior to printing, the blue channel of the character sequence was modulated with a gain $w_{B_i} = 1$ (no color alteration) for odd i, $i = 1, 3, \ldots, K-1$, and with a gain $w_{B_i} = 0.81$ for even i, $i = 2, 4, \ldots, K$. Using these values, empirical tests indicate that it is hard for a human observer to distinguish between a modulated and a non-modulated character. In this case, according to the perceptual distortion metric described in (12), the distortion is given by $D = 34.67$. In fact, the empirical tests performed with human observers have illustrated that $D < 40$ are usually not perceivable by the human eye.

The elements with no color alteration ($w_{B_i} = 1$) carry bit 0, and the elements modulated with $w_{B_i} = 0.81$ carry bit 1. The task is to classify each printed character as having a bit 0 or bit 1 embedded into it. In this example, the difference $d_b = d_B - d_G$ is used as a detection metric, as given in (5).

To retrieve the embedded information, the document is scanned and the text is segmented from the background using simple thresholding. Segmentation errors are not observed in this set of tests, however it is clear that they may cause synchronization detection errors. The use of channel coding is an efficient option to reduce the bit errors caused by wrong segmentation [6].

The histogram of the detection results are presented in Fig. 6. The error rates for this experiment are presented in Table 1, in the row corresponding to d_b. For comparison, this table also presents error rates using simple TLM, where the three channels are modulated with the same gain, simulating a single-channel gray level modification only. With the same equipment and resolutions, the modulation gains

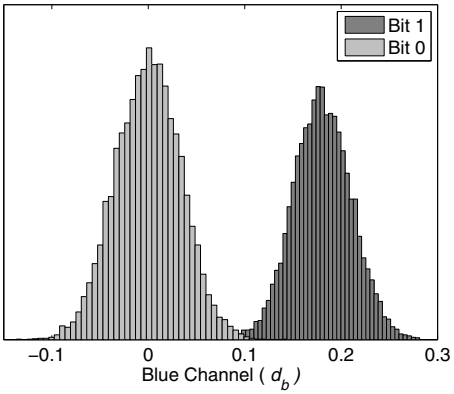

Figure 6. Histogram of the detection metric d_B, for the blue channel.

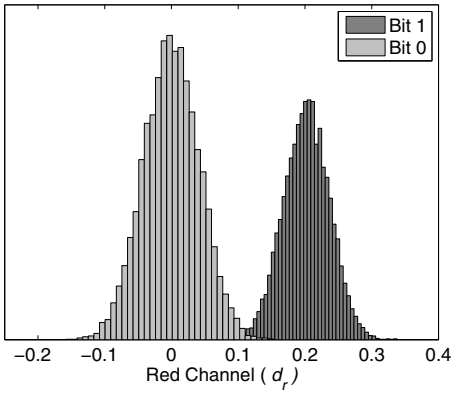

Figure 7. Histogram of the detection metric d_R, for the red channel.

for TLM was 0.81, which causes $D = 39.59$, also making the modulation hard to perceive. The modulation level using TLM was evaluated using only the average luminance as a detection metric. Although additional metrics can be used in TLM (variance and higher order statistics, as discussed in [4]), these additional metrics can also be applied in TCM. Notice that color modulation presents a lower error rate in comparison with simple luminance modulation.

7.2. Experiment 2: Red Channel Modulation

This experiment is similar to Experiment 1, however the red channel is modulated, with a gain $w_{R_i} = 0.85$ for $i = 2, 4, \ldots, K$. This gain value was modified such that the distortion D remained the same as in Experiment 1, that is, $D = 34.67$. In this example, the difference $d_r = d_R - d_G$ is used as a detection metric, as described in (5). The histogram of the detection results and the error rates for this experiment are given in Fig. 7 and Table 1, respectively. Notice that when no modulation is performed (bit 0), no difference between the averages of the red and green channels is expected, in agreement with the experimental results.

7.3. Experiment 3: Combined Blue-Red Channel Modulation

In this experiment, the blue and the red channels are modulated in characters c_i, $i = 2, 4, \ldots, K$. The modulation gain is given by $w_B = 0.76$ and $w_R = 0.88$, which are the modulation values that yield the minimum distortion for an error probability equal to 0.0001, according to the result presented in Figure 4. In this case, the distortion of the modulated characters is given by $D = 39.03$.

Detection Type	Number of Errors	Error Rate
TLM	139	4.6×10^{-3}
Blue Modulation (d_b)	35	1.2×10^{-3}
Red Modulation (d_r)	53	1.7×10^{-3}
Red-Blue Modulation ($\mathbf{d_2}$)	6	1.96×10^{-4}
Orientation (d_a)	1040	3.39×10^{-2}
Red-Blue-Orientation ($\mathbf{d_3}$)	2	6.59×10^{-5}

Table 1. Experimental error rates for TCM and TLM.

In the detection, the information from the blue and red channels are combined according to the Bayes classifier, as described in Section 3.3. Fig. 8 shows a scattered plot with the decision function obtained for this set of tests.

The experimental error rates combining the two channels with the Bayes classifier is given in Table 1, in the row corresponding to $\mathbf{d_2}$. This illustrates that the detection using two color channels is more efficient than single channel detection, at the expense of a slight increase in the distortion. However, this distortion is still hardly perceived by a human observer.

7.4. Experiment 4: Auxiliary Angular Detection

This experiment presents the improved performance using the approach described in Section 6, where the average energy d_a of the output of the directional filter f_{dir} is used as a detection metric. The experiments illustrate that when d_a is used alone, it does not bring an error rate as low as the metrics d_b and d_r, as shown in Table 1. However, d_a can be combined with d_b and d_r used in Experiments 1 and 2 us-

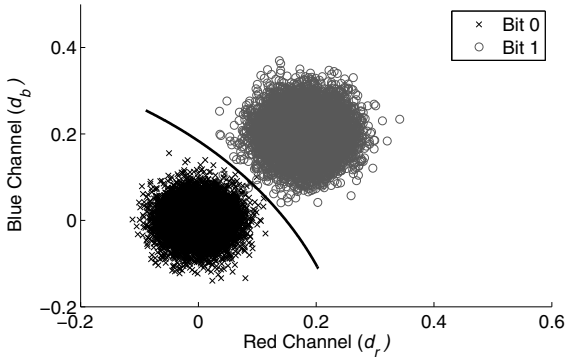

Figure 8. Scatter plot illustrating curve separating the detection values for bit 1 and bit 0.

ing the Bayesian approach, to help reducing the error rate. Results using this approach are also given in Table 1, in the row corresponding to $\mathbf{d_3}$.

Fig. 9 shows a 3-D plot showing a surface separating the modulated from the non-modulated characters. The directional filter used in this example was oriented at $165°$, which corresponds to the cyan screen angle plus $90°$. As the predominant screen used to represent blue is the cyan (although it is mixed with magenta for plain blue and with the other colors for dark blue), $165°$ is the filtering angle which outputs the greatest energy. Notice that for devices which use different printing angles/halftoning algorithms, an evaluation of the angular/texture properties is necessary before applying this detection metric.

7.5. Experiment 5: Variable Modulation Gains

This experiment extends 'Experiment 3' by observing the error rates for different gains in the red-blue channel modulation case. Instead of testing only for $w_{B_i} = 0.76$ and $w_{R_i} = 0.88$, $i = 2, 4, \ldots, K$ (even i), the tested gains are $w_{R_i} = w_{B_i} = 0.97$, $w_{R_i} = w_{B_i} = 0.9$, $w_{R_i} = w_{B_i} = 0.84$, for even i. The goal of this experiment is to evaluate how accurate is the upper bound on the error rate compared to practical results.

Fig. 10 shows a plot with the theoretical (full line) upper bound on the error probability described by (11) derived in the analysis of Section 3, as a function of the gain $w_R = w_B$. Because $w_R = w_B$, a two-dimensional plot is used to illustrate the errors, instead of the 3-D plot shown in Fig. 2. Figure 10 also shows the experimental error rates (represented by crosses) as a function of the difference between the original character luminance and the gain $w_{B,R}$. This figure indicates the similarity between the theoretical and the experimental results after printing and scanning.

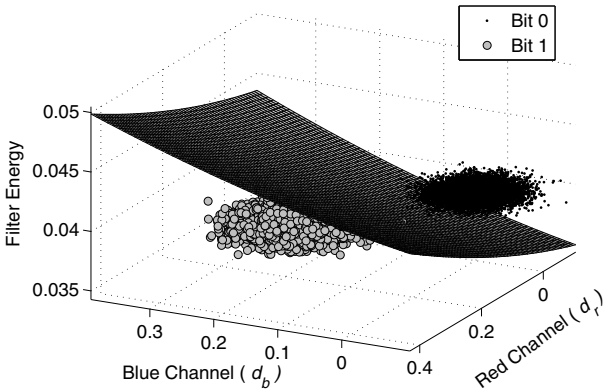

Figure 9. Plot illustrating surface separating the detection values for bit 1 and bit 0, using d_b, d_r and d_a as detection metrics.

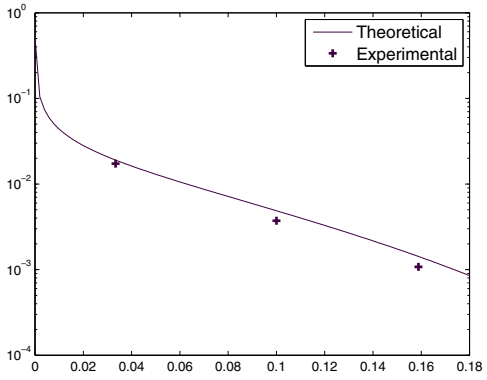

Figure 10. Error probability for different gains, using $w_B = w_R = 0.97, 0.9, 0.84$. The horizontal axis indicates the luminance difference between the original and the modulated character, for the red and blue channels. The full line represents the theoretical error rate derived in Section 3, the cross dots represent the experimental error rates after PS.

8. Conclusions

This paper has discussed TCM, a practical method for text data hiding. It proposes a new detection approach, where the information from the blue and red channels is used to detect the embedded information. The proposed detection uses the difference in the pixel averages between the blue and the green channels and the difference in the pixel averages between the red and the green channel. An error rate analysis is presented considering the detection using the blue and red channels separately. An upper bound on the error rate for the case where the blue and red channel information is combined is also presented. The analysis are performed based on a PS channel model, which is described in the paper.

The proposed detection also uses the orientation characteristics of color halftoning to reduce the error rate. Because color halftoning algorithms use different screen orientation angles for different color channels, this is used as an effective feature to detect the embedded message.

In addition, this paper also uses a perceptual color distortion model which is used to determine the optimum modulation values for a given detection error probability.

Experiments illustrate the applicability of method and the superior performance of the use of color over simple TLM.

References

[1] International Commission on Illumination (CIE) in *Recommendations on uniform color spaces, color diference equations, psychometric color terms,* Publication CIE 15 (E.-1.3.1), Supplement No.2, Bureau Central de la CIE, Vienna, 1971.

[2] F. Baqai, J. Lee, A. Agar, and J. P. Allebach. Digital color halftoning. *IEEE Signal Processing Magazine*, 22(1), January 2005.

[3] P. V. K. Borges and J. Mayer. Document watermarking via character luminance modulation. In *IEEE International Conferenc on Acoustics, Speech and Signal Processing, ICASSP*, Toulouse, France, May 2006.

[4] P. V. K. Borges and J. Mayer. Improving robustness in printed side communications using higher order statistics. In *IEEE International Conferenc on Acoustics, Speech and Signal Processing, ICASSP*, Honolulu, Hawaii, USA, April 2007.

[5] P. V. K. Borges and J. Mayer. Text luminance modulation for hardcopy watermarking. *Signal Processing*, 87(7), 2007.

[6] M. C. Davey and D. MacKay. Reliable communication over channels with insertions, deletions, and substitutions. *IEEE Trans. on Inf. Theory*, 47, 2001.

[7] N. Degara-Quintela and F. Pérez-González. Visible encryption: Using paper as a secure channel. In *Proceedings of SPIE: Security and Watermarking of Multimedia Contents V*, volume 5020, Santa Clara, CA, USA, 2003.

[8] F. Deguillaume, S. Voloshynovskiy, and T. Pun. Character and vector graphics watermark for structured electronic documents security, September 2004. US Patent Application 10/949,318.

[9] R. O. Duda, P. Hart, and D. G. Stork. *Pattern Classification*. John Wiley, 2nd edition, 2001.

[10] G. Langelaar, I. Setyawan, and R. Lagendijk. Watermarking digital image and video data. *IEEE Signal Processing Magazine*, 2000.

[11] P. Lennie. Color vision: putting it together. *Current Biology*, 10(16), 2000.

[12] R. Víllan, S. Voloshynovskiy, O. Koval, and T. Pun. Multilevel 2d bar codes: towards high capacity storage modules for multimedia security and management. In *Proceedings of SPIE Photonics West*, San Jose, CA, USA, January 2005.

[13] R. Víllan, S. Voloshynovskiy, O. Koval, J. Vila, E. Topak, F. Deguillaume, Y. Rytsar, and T. Pun. Text data-hiding for digital and printed documents: theoretical and practical considerations. In *Proceedings of SPIE-IST Electronic Imaging*, San Jose, CA, USA, 2006.

[14] X. Zhang and B. A. Wandell. Color image fidelity metrics evaluated using image distortion maps. *Signal Processing*, 70(3):201–214, November 1998.